Microwave Assisted HMDSO/Oxygen Plasma Coated Polyethylene Terephthalate Films: Effects of Process Parameters and Uniaxial Strain on Gas Barrier Properties, Surface Morphology, and Chemical Composition

Ernst Schmachtenberg,[1] Francis Reny Costa,[2] Sebastian Göbel[1]

[1]*Institut für Kunststoffverarbeitung Aachen, 52062 Aachen, Germany*
[2]*Rubber Technology Center, Indian Institute of Technology, Kharagpur 721302, West Bengal, India*

Received 22 March 2004; accepted 17 July 2004
DOI 10.1002/app.21266
Published online in Wiley InterScience (www.interscience.wiley.com).

ABSTRACT: The coating structure and barrier property relation of coated PET films is of high interest for understanding the difference between predicted and actual barrier performance of coated PET films. In this work the chemical and morphological structure of HMDSO coatings generated with and without oxygen in a microwave plasma has been investigated with XPS and AFM analysis. These results were correlated with oxygen permeation measurements at different strain rates and temperatures. The results show that with a more glass-like chemical composition the barrier property is improved. The growth of the coatings takes place in a columnar manner and the interfaces between the columns seem to be the low energy passages for the permeation, which cause the difference between predicted and actual barrier performance. When the coatings are strained the barrier fails at a strain higher than 1%. Cracks occur and with higher strain rates the number of cracks increases. Cracking takes place perpendicular to the strain direction and at the interfaces of the columns of the coating. © 2005 Wiley Periodicals, Inc. J Appl Polym Sci 99: 1485–1495, 2006

Key words: plasma polymerization; gas permeation; structure–property relations; thin films

INTRODUCTION

The low gas barrier property of polymers is a serious limitation of many conventional polymers for their application in packaging industries. Therefore, improvement of the barrier property of these polymers in terms of both extent and longevity has always remained a very specific issue. Transparent glass-like barrier coatings on thin polymeric films or on the surfaces of blow-molded articles are gaining more importance in various industries such as packaging, pharmaceuticals, biomedical, etc. Plasma enhanced chemical vapor deposition (PECVD) has already been established as an efficient method to produce very thin and homogeneous coatings on an extremely wide range of polymer substrates.[1–5] Typically, thin SiO_x type coatings obtained from a plasma containing oxygen and a silicon organic precursor gas could improve the barrier properties by a large extent. However, PECVD is a complex process that involves a large number of critical process parameters, which directly influence the nature and hence the performance of the barrier coating. Therefore, a clear understanding of the effects of these process parameters on the physical and chemical nature of the coatings is always important. Again, the deposition of an efficient barrier coating does not necessarily guarantee satisfactory performance of the laminates in service. The coating layer should also be tough enough to sustain its structural integrity against various kinds of stress to which it is subjected during the fabrication processes or the usage.

Among the various factors that determine the barrier efficiency of the coatings obtained by PECVD, coating layer thickness, nature and density of the defects, chemical composition, and nature of packing of the structural units of the coating layers are the most significant ones. It is now well known that gas permeation decreases with increasing coating thickness when the latter exceeds a certain critical value.[4,6,7] Additionally the surface roughness of the coating seems to have a significant effect on the permeation rate.[8–10] Generally the SiO_x coatings do not have the barrier performance expected from theoretical considerations.[11] This is caused by defects in the coating, which are the major low energy passages for the permeant molecules that account for residual gas permeance through the coating layer. Rossi and Nul-

Correspondence to: S. Göbel (goebel@ikv.rwth-aachen.de).
Present address for F. R. Costa: Institut für Polymerforschung, Hohe Strasse 6, 01069 Dresden, Germany.

man,[12] Sobrinho et al.,[7] and Roberts et al.[11] have developed theoretical models that describe the influence of the defect geometry, defect size, and the defect density on permeation through the coating layer. It has been reported that permeation through coating layers increases with increasing both density and size of the defects. They have also shown that a high density of microdefects (pinholes) causes more permeation compared to a low density of large defects when the fractions of the coated surface area covered by defects are comparable in both cases.

The analysis of AFM and SEM micrographs of SiO_x and AlO_x type coatings have revealed that the deposition of the particles takes place in either columnar[13] or granular[14–17] form. These defects have been made visible by several preparation techniques. In TEM micrographs (usually top view) it seems that the defects are at the interface between two columns/grains. With another technique (confocal microscopy) the defects are only indirectly accessible, thus a conclusion of the morphology of the defects may not be drawn.

The chemical composition of the coating is always a very important factor that determines the efficiency of the barrier layer. In a SiO_x type of barrier coating it has been observed that barrier properties improve as the x value approaches 2 and as the proportions of carbon and hydrogen in the coating layer decrease.[2,4,18]

The effect of strain on coated films was first studied by Felts.[19] He found that the barrier properties remain nearly unchanged up to critical strain. Above this strain he found a serious loss in the barrier performance. Heil[2] mentions in this context that the strain rate has a significant influence on the critical strain.

In the present study SiO_x barrier layers on PET films have been deposited using a hexamethyldisiloxane (HMDSO)/oxygen plasma excited by a microwave energy source in contrast to the usual RF or HF excitation. The effects of microwave power input and oxygen flow rate during the coating process on the surface morphology, the chemical composition, and the oxygen barrier property have been studied. An attempt has been made to study how uniaxial strain affects the SiO_x type barrier layer.

EXPERIMENTAL

Materials

For our studies a 12-μm-thick PET film was used (supplied by Hoechst Diafoil GmbH). Hexamethyldisiloxane used as precursor monomer was of synthetic grade with 98% purity and specific gravity 0.76 (supplied by Sigma–Aldrich Chemie GmbH). The oxygen used was of 99.995% purity and the nitrogen used as carrier gas for the permeation measurements contained, besides N_2, 95 ppm O_2 and 1.75 mol % H_2 (all gases supplied by Linde AG).

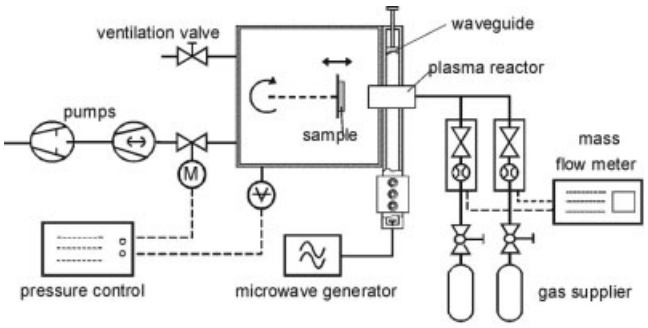

Figure 1 Sketch of the plasma reactor used for coating PET films.

Experimental setup

The reactor used was of a downstream plasma reactor type, i.e., the substrate to be coated was kept outside the plasma volume. Figure 1 shows the plasma reactor used for coating PET films. It consists of a vacuum chamber containing a rotatable sample holder, a vacuum pump with a pressure controller, a mass flow controller, and a microwave generator (1.2 kW, 2.45 GHz) with a wave-guide system and integrated plasma source.

Microwave power input and the oxygen flow rate into the plasma reactor for coating one side of the PET films were varied as shown in Table I. Other process parameters, namely microwave frequency, pressure, coating time, distance between the substrate and the plasma region (Fig. 1), and the HMDSO flow rate were kept constant as follows:

1. Microwave frequency: 2.45 GHz
2. Pressure: 20 Pa
3. Coating time: 30 s
4. Distance from plasma: 50 mm
5. HMDSO flow rate: 10 sccm (standard cubic centimeter)

PET films were cut into square pieces, fixed on the substrate holder of the plasma reactor, and rotated during plasma coating to ensure equal exposure of the film surface to the flux of various reactive species from the plasma region. For coating both sides of the substrate, sufficient time was allowed after coating of one side to bring it to room temperature and then the other side was coated using similar conditions.

Measurement of oxygen permeation

The oxygen permeance through both coated and uncoated PET films was measured using an Ox-Tran 100A (Modern Controls Inc.). The area of the sample chamber was 100 cm^2. Since the uniformly coated region on PET film is smaller than the area of this

TABLE I
Experimental Set-ups for the Coating Process

Sample no.	HMDSO flow rate (sccm)	Oxygen flow rate (sccm)	Pressure (Pa)	Time of deposition (s)	Distance (d) (mm)	Power (W)
A1	10	0	20	30	50	300
A2	10	50	20	30	50	300
A3	10	100	20	30	50	300
A4	10	200	20	30	50	300
A5	10	0	20	30	50	400
A6	10	50	20	30	50	400
A7	10	100	20	30	50	400
A8	10	200	20	30	50	400
A9	10	0	20	30	50	500
A10	10	50	20	30	50	500
A11	10	100	20	30	50	500
A12	10	200	20	30	50	500

sample chamber, films were masked with self-adhering aluminum foil leaving the central portion (a circular area of diameter 25 mm) of the coated surface exposed for gas permeation. To measure the oxygen permeance through the films under strain, a metallic frame (Fig. 2) was used. The films were fixed on this frame and given a certain amount of strain before setting them in the chamber of the Ox-Tran. A more detailed description of the measurement device is given in Michaeli et al.[20] All oxygen permeation rate measurements were carried out at a constant temperature of 35 ± 1°C, if not specified. The oxygen was saturated with water vapor at 20°C and then heated to the actual measurement temperature, thus the absolute humidity was kept constant.

Chemical compositions of the coating layer

Chemical compositional analysis of the coating layer was carried out using a XPS (M-Probe, Surface Science). Relative chemical composition of the coating layers was calculated from the characteristic peak intensity ratio. The nature of the chemical environment of the Si atom in the coating layer was evaluated from the binding energy of the Si(2p) and Si(2s) orbitals.

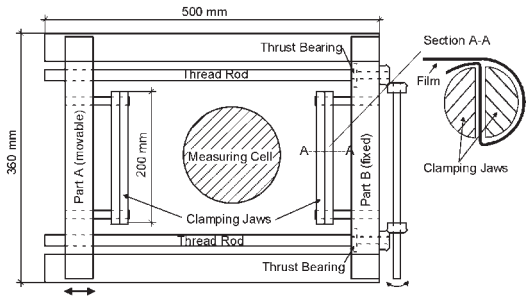

Figure 2 Metallic frame with movable clamp used for stretching films during the oxygen permeance measurement in the Ox-Tran 100A.

Surface morphology of the coating layers

To study the surface morphology of the coating layer, tapping mode AFM (Digital Instruments Dimension 3100 AFM, AC160TS cantilever), TEM (Zeiss EM 900), and SEM (Zeiss DSM 960A) were used. For the AFM study, the coated films were fixed on a metallic frame, which was used to impart strain to the film. The frame was then mounted on the sample holding platform under the scanning head in the AFM instrument. For investigating the nature of the strained surface under the SEM, the coated film was strained first and then an adhesive tape was fixed on the uncoated side of the strained film to maintain the strain. A small square piece of such an attachment was then cut and coated with gold for SEM study. Though this was a crude method of sample preparation, as the exact strain level could never be maintained, some interesting observations were made from the SEM photographs that will be discussed in the following sections.

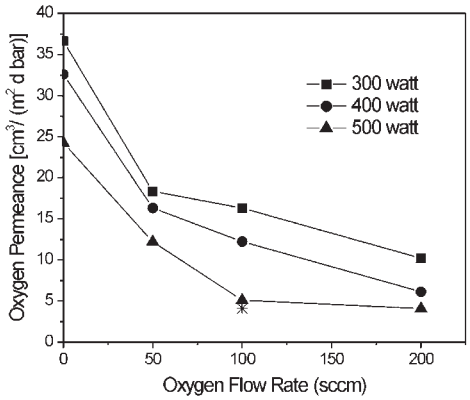

Figure 3 Variation of oxygen permeance of the single-side–coated PET film (SiO_x/PET) with oxygen flow rate and microwave power input. *The permeance of both-side–coated PET film obtained using the parameter set A9, i.e., oxygen flow rate = 100 sccm and microwave power input = 400 W.

RESULTS AND DISCUSSION

Oxygen permeation

The uncoated 12-μm-thick PET film showed an oxygen permeance value of 53 $cm^3/(m^2\ d\ bar)$, while the single-side coated films (represented as SiO_x/PET) expectedly showed a lowering of this value though not to a large extent. However, it is possible to obtain a very efficient SiO_x barrier coating using the PECVD technique with lowering of oxygen permeance by two orders of magnitude.[3] The PET film coated on both sides (prepared using the coating condition of sample A9 and represented as SiO_x/PET/SiO_x) shows further lowering of the oxygen permeance value. Figure 3 shows that the oxygen permeance through SiO_x/PET decreases when the oxygen flow rate and microwave power input increase during the plasma coating process. To explain this trend understanding of the changes that occur in the chemical composition and the surface morphology of the coating layer is essential. This will be described in subsequent sections.

Chemical analysis

The chemical analysis of the coating layers were studied using XPS. Since peak areas in XPS spectra are directly proportional to the atomic concentration of the respective element,[21] the ratio of two different peak areas could be used to indicate the relative proportions of the two elements in the coating layers. Again, the binding energy (BE) of a particular orbital of any element is a clear indicator of its chemical environment. So, the trends in the BE of Si(2s) and Si(2p) orbitals were used to indicate the change in the chemical environment of Si atoms in the coating layers. Figure 4(a–c) shows the variation in various atomic ratios in the coating layers. It is evident from this figure that, as the oxygen flow rate and microwave power input increase, the inorganic nature of the coating layers increases. The comparisons of these atomic ratios with those present in HMDSO and polydimethyle siloxane (PDMSO, $-[(CH_3)_2SiO]_n-$) show that the carbon contents in the coating layers are much lower. The Si/O ratio close to 0.5 indicates the closer similarity to silica glass. Figures 5 and 6 show the XPS peaks for the Si(2p) and Si(2s) orbitals and their variation with microwave power and oxygen flow rate. The binding energies of the Si(2s) and Si(2p) orbitals increase as the microwave power input and oxygen flow rate into the plasma reactor are increased and approach those obtained in silica glass. Similar types of observations have also been made by other researchers.[4,22] The lowering of the carbon content and the increasing inorganic nature of the coating layers certainly improve their oxygen barrier properties.[4,23]

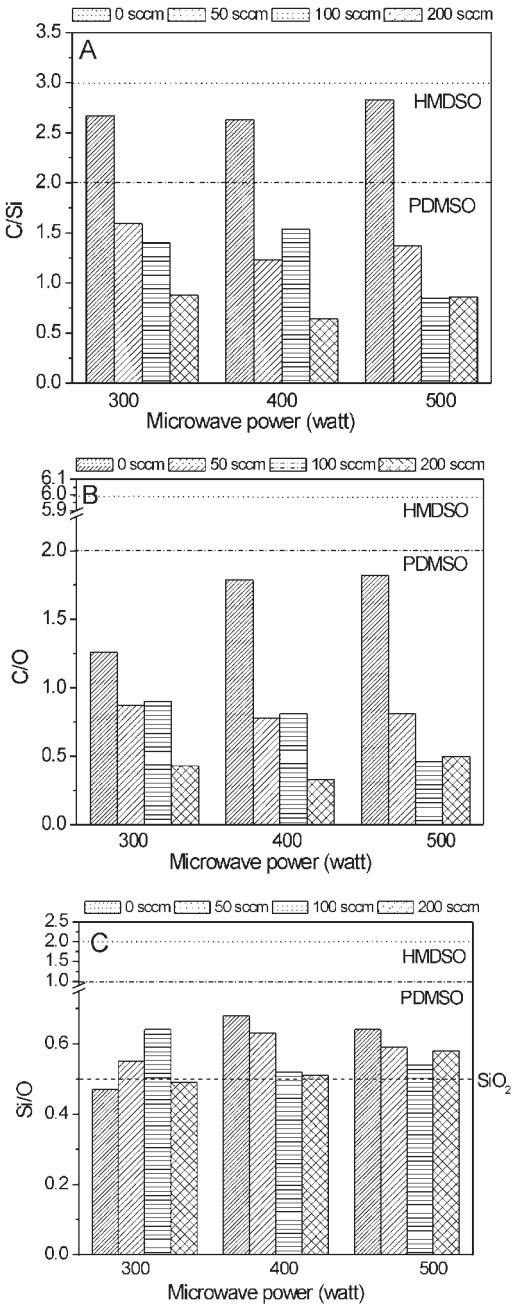

Figure 4 The effects of process parameters on the chemical composition of the coating layer.

Surface morphology

The TEM micrograph of the cross section of coating layer obtained from HMDSO/O_2[27] plasma reveals that the thickness develops through columnar growth of the deposited particles (Fig. 7).[28] The interfaces between the single columns (diameter 80 nm) are possibly the nanodefects described in Roberts et al.[11] and may be the possible cause for the poor barrier performance of the coated films. However, with the increasing oxygen flow rate and microwave power input, the surface roughness and the defects density decrease,

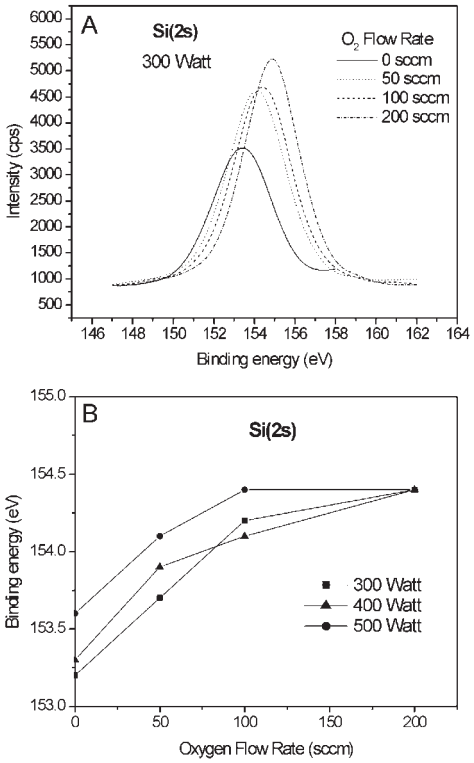

Figure 5 Effects of process parameters on the binding energy of silicon atomic orbital in the coating layer: (a) ESCA peaks for Si(2s) orbital; (b) variation of Si(2s) binding energy.

which accounts for the lowering of oxygen permeability. Figure 8 shows that the packing of the deposited particles becomes more compact with increasing oxygen flow rate during the coating process. This could be due to the higher degree of fragmentation of the HMDSO molecule and its fragmented products, which reduces the deposition of large particles and their shadowing effect after deposition.

Activation energy of oxygen permeation and mechanism of permeation

In this section, activation energy of oxygen permeation through both coated and uncoated PET films has been calculated following activated rate theory[3,24] for the temperature dependence of the permeation. According to this theory the permeation of noninteracting gases through glassy polymers below their glass transition temperature is given by

$$\prod = \prod_{o} e^{-(E_P/RT)} \tag{1}$$

where Π is the permeance ($cm^3/(m^2\ d\ bar)$), Π_o is a constant unique to the system, E_P is the apparent activation energy (J/mol) of oxygen permeation, R is the universal gas constant (J/mol K), and T is the absolute temperature (K).

For a multilayer barrier system, like the present case, the above equation can be expressed as[3]

$$\prod_{12\ldots} = \left[\frac{e^{E_{P1}/RT}}{\prod_{o_1}} + \frac{e^{E_{P2}/RT}}{\prod_{o_2}} + \ldots\right]^{-1} \tag{2}$$

Equation (2) expresses that each layer in the laminate barrier structure contributes to the total energy required for permeation and the layer the having highest value of E_P/RT in eq. (2) determines the activation energy for the whole system. Therefore, any physical and chemical change in that layer will be reflected in the value of the overall activation energy (E_P) for the laminate.

In this work, we studied three different barrier systems, such as uncoated PET films, one-side–coated PET films (SiO_x/PET), and double-side–coated PET films (SiO_x/PET/SiO_x). To calculate the activation energy of oxygen permeation through them, oxygen permeances at four different temperatures were measured. The activation energy values are shown in Figure 9. The uncoated PET and the one-side–coated PET films show similar E_P values as those reported in literature.[3,8] This similarity in the activation energy indicates that the low energy passages for the permeant molecules are similar

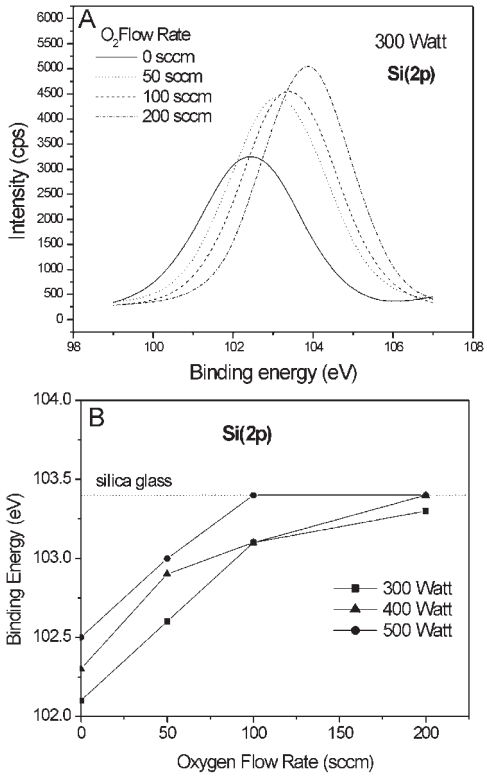

Figure 6 Effects of process parameters on the binding energy of silicon atomic orbital in the coating layer: (a) ESCA peaks for Si(2p) orbital; (b) variation of Si(2p) binding energy.

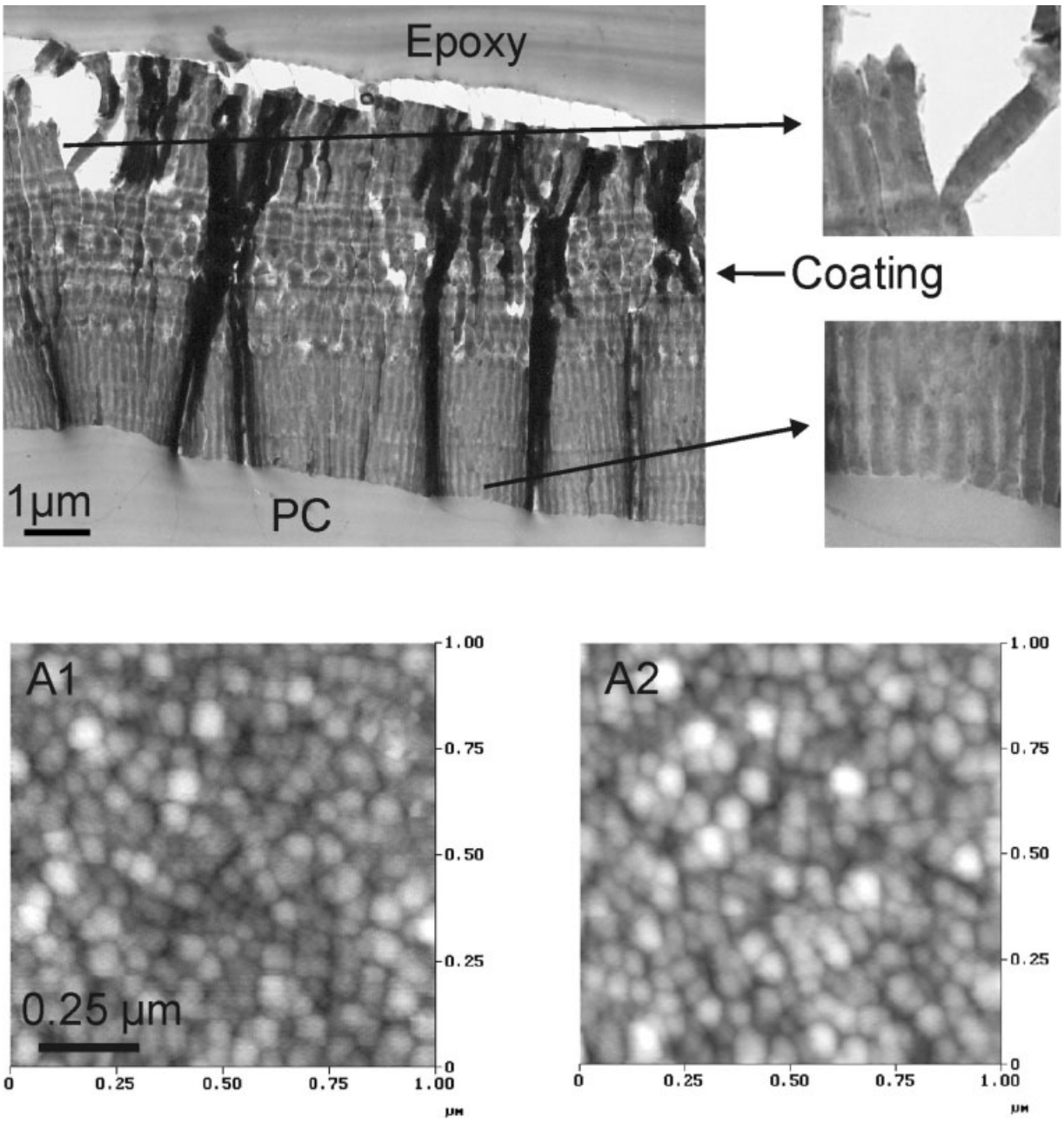

Figure 7 Microstructure of the coating layer obtained from HMDSO/O_2 plasma. (Top) TEM image showing nature of growth of the layer; (bottom) AFM image showing surface morphology (A1- HMDSO plasma and A2- HMDSO/O_2 plasma).

for both the systems and the coating architecture does not have any significant influence on the temperature dependence of the permeation process. Nevertheless, the probability of the permeant molecules diffusing through the defect-free regions of the coating layers cannot be considered to be zero. When this probability is very small compared to the probability of diffusion through defects, the diffusion through the coating layer will not have any contribution to the activation energy of the permeation process. In this situation, the bulk of coating simply acts as a "block," which permeant molecules must bypass until they find the defects and get access into the PET layer.[3] As a result, the coated film will show an activation energy value similar to that of uncoated PET film.

The activation energy of the both-side–coated film was found to be much higher than that of the uncoated and the single-side–coated films. This type of observation was also made by Tropsha et al.[3,25] in the case of RF-assisted plasma (in presence of organo silicon monomer and oxygen) coated PET films. Moreover, the activation energy they obtained was much higher than that obtained in this work. This may be due to the differences in the coating processes, which

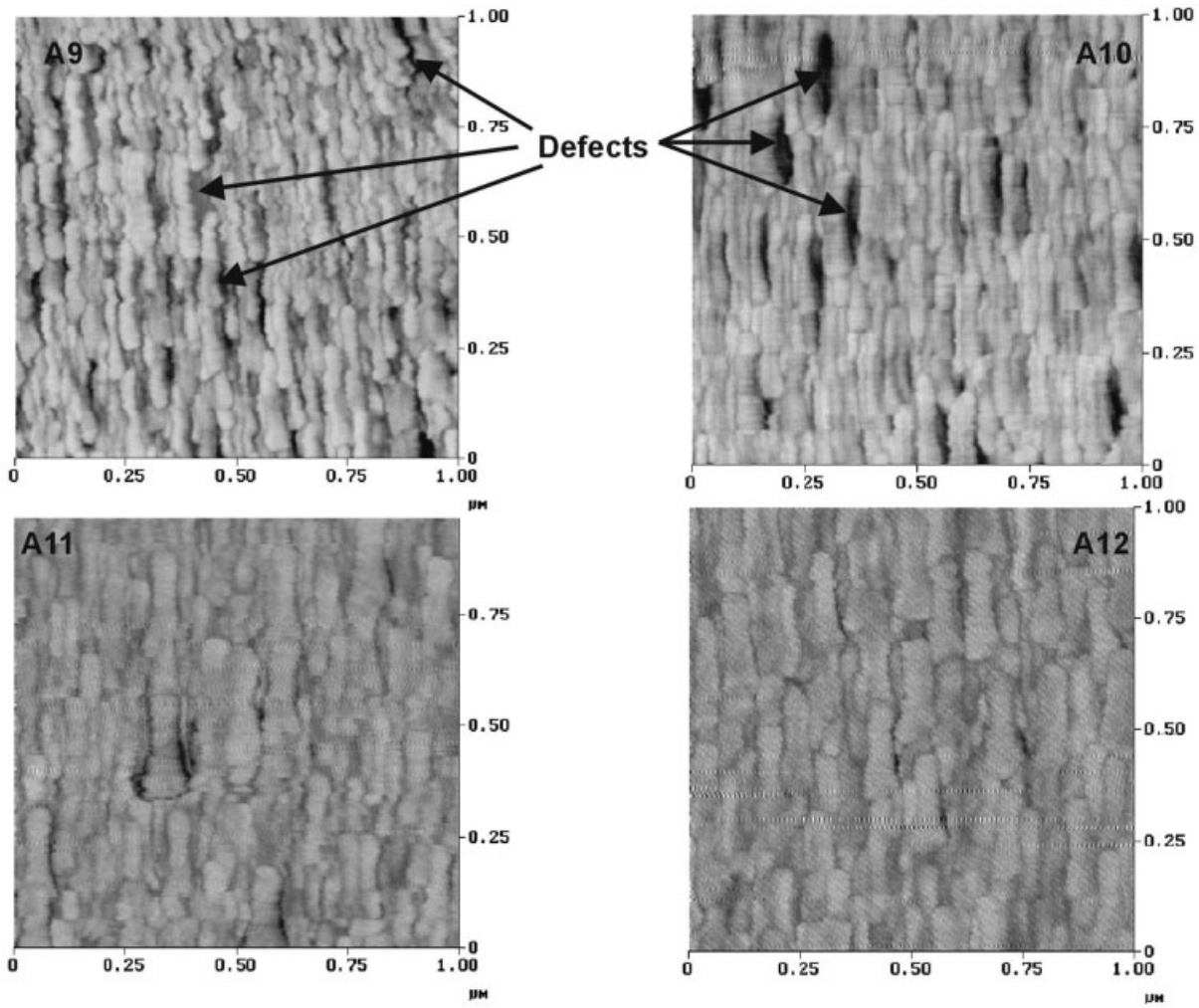

Figure 8 Effects of oxygen flow rate on the surface morphology of the coating layer, microwave power 500 W, oxygen flow rate (A9) 0 sccm, (A10) 50 sccm, (A11) 100 sccm, and (A12) 200 sccm. R_{ms}: A9 = 1.6, A10 = 1.5, A11 = 1.5, A12 = 1.4; R_a: A9 = 2.0, A10 = 1.9, A11 = 1.8, A12 = 1.8.

certainly change the chemistry and surface morphology of the coating layers. However, the model they proposed to explain the increase in the activation energy in case of the both-side–coated film is equally applicable in this case. It is expected that the nature and thickness of coating layers are similar on both sides of the PET film in a SiO_x/PET/SiO_x system. Figure 10 shows the various models describing the ways by which permeant molecules may permeate through the both-side–coated film. In model "a" permeant molecules find the defects in the coating layer on the both sides of the PET film (path 1). Such a situation will result in an activation energy of the permeation similar to that of the uncoated PET film. In models "b" and "c" the permeant molecules permeate solely through the defect free regions of the coating layer at least on one side of the films (paths 2, 3, and 4). Thus, in these cases, SiO_x type coating layers will be rate determining for the permeation process and the activation energy will be decided by the nature of the defect-free region of the coating layer. This means that the presence of defects in the coating layers will not have any effect on the temperature dependence of the permeation process, despite the fact that permeant molecules always prefer low energy passages such as various kinds of defects. Therefore, models "a" and "b" cannot represent the actual situation as they directly contradict the established fact that kinetics of permeation process depends on density and nature of defects.[6,12] In this context, model "a," although it gives the lowest energy mechanism for oxygen permeation, cannot explain the high activation energy for the SiO_x/PET/SiO_x system. Again the probability of finding the defects by the permeant molecules on the second coating side (where desorption occurs) is not 1; so it may happen that some of them diffuse through the defect-free regions of the coating layer due to the unavailability of low energy passages very close to their path of diffusion. This tendency of the permeant molecules will be increasingly prevalent with the de-

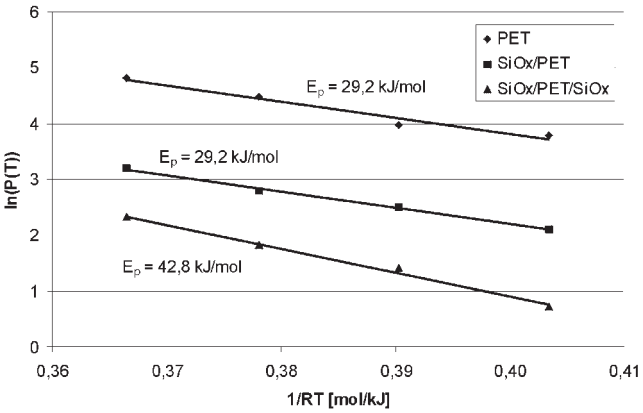

Figure 9 Arrhenius plot for the calculation of the activation energy of oxygen permeation through coated and uncoated PET films.

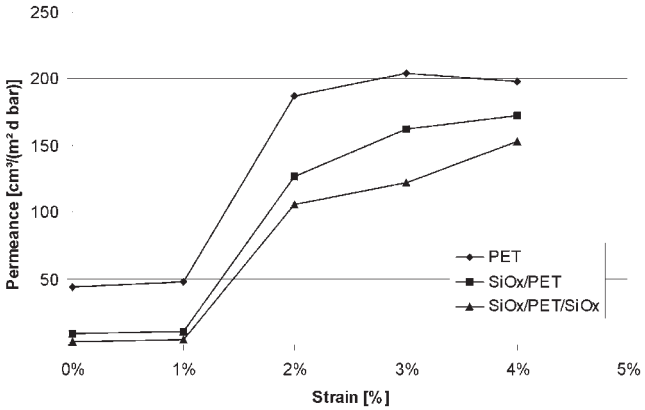

Figure 11 Variation of the oxygen permeance through barrier layers with uniaxial strain.

creasing defect size and defect density in the coating layer. This has been illustrated in model "d" in Figure 10, where all four types of possible paths are shown operating. The relative proportion of these paths followed by the permeant molecules will decide the final barrier improvement in terms of permeance and activation energy. When paths 2, 3, and 4 altogether are insignificant compared to path 1, the activation energy of the coated films will be similar to that of the uncoated PET film, but the permeance will be lower because the coating layer, even if having a large number of defects, always acts as a block toward the diffusion of permeant molecules. But when at least any of the paths 2, 3, and 4 becomes appreciable, the activation energy will be higher and, as their proportions increase, it will approach that of the defect-free coating layer. For the present work model "d" of Figure 10 was considered and accordingly the behavior of the coating layers with unidirectional strain is explained.

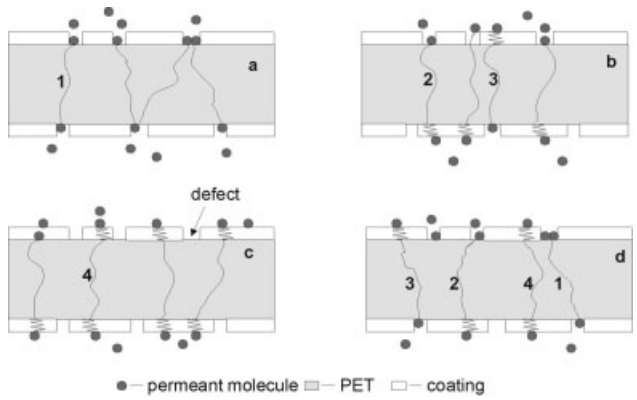

Figure 10 Models showing the probable ways of gas permeation through both-side–coated films; numbers indicate the type of path: 1, through PET alone via defects; 2 and 3, through defect-free coating region on one side and defect on the other side; 4, through defect-free coating region on both sides of PET film.

Effect of uniaxial strain on barrier coating layer

Oxygen permeation

In all coated and uncoated films oxygen permeance increased with increasing strain in the film (Fig. 11). There was no significant change in the oxygen permeance up to 1% strain, but from 1 to 2% strain, the oxygen barrier property failed with abrupt increase in the permeance. The same observations were made by Yanaka et al.[26] on electron beam evaporated SiO_x coated PET films. At a strain higher than 2%, the rate of increase in permeance again slowed down and the SiO_x/PET/SiO_x system always showed better barrier performance than SiO_x/PET and PET. The strain rate is an extremely important aspect that has to be considered while doing these kinds of studies, especially when comparing the results of similar kinds of investigations from different sources.[2,19] Besides this, the direction of stress with respect to the extrusion direction of the original PET film may influence the results. Therefore, the critical strain at which the gas barrier

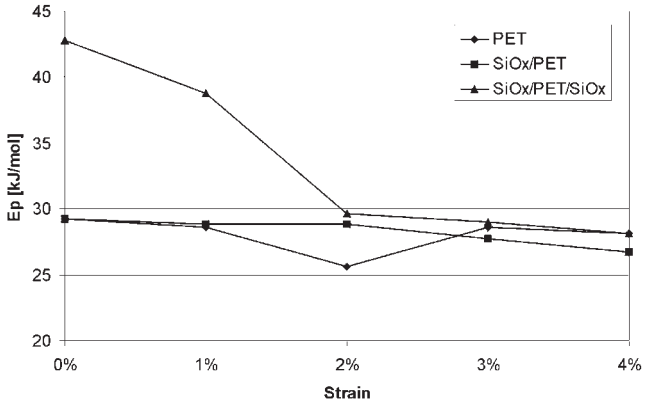

Figure 12 Variation of the activation energy (ΔE_p) of the oxygen permeation through barrier layers with uniaxial strain.

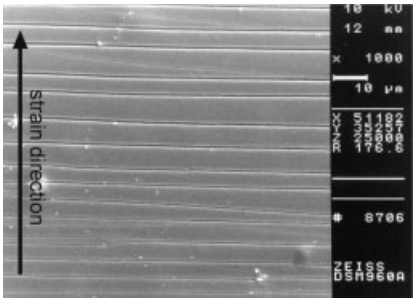

Figure 13 SEM image of the surface of the strained single-side–coated PET film (strain is around 2%).

property of any SiO_x type of coating fails cannot be inferred as unique for any pair of substrate and coating layer unless all the parameters influencing it, such as coating thickness, coating chemistry, strain rate, etc. are maintained constant. In the present study, every attempt was made to keep the strain rate low and nearly constant. The direction of stress was chosen deliberately perpendicular to the direction of PET film extrusion, which apparently seems the weaker direction as far as the strength of the films is concerned.

The activation energy of oxygen permeation (E_p) shows no significant change with strain in cases of PET and SiO_x/PET. However, in SiO_x/PET/SiO_x, E_p decreases sharply up to 2% and, above that strain, E_p values of these three barrier systems become comparable (Fig. 12). The decreasing trends in the activation energy can be explained by model "d" in Figure 10. The similarity in the E_p values of PET and SiO_x/PET type barrier indicates that the permeant molecules follow path numbers 1 and 2 (Fig. 10), preferably in the latter. For the both-side–coated films (SiO_x/PET/SiO_x) the much higher value of E_p indicates that there is a significant number of permeant molecules that follow paths 3 and 4 (Fig. 10). When films are strained, cracks appear (Figs. 13 and 14) and the number of defects on the coating layer increases. As a result, the number of molecules following the high-energy path decreases with increasing strain and so does the E_p

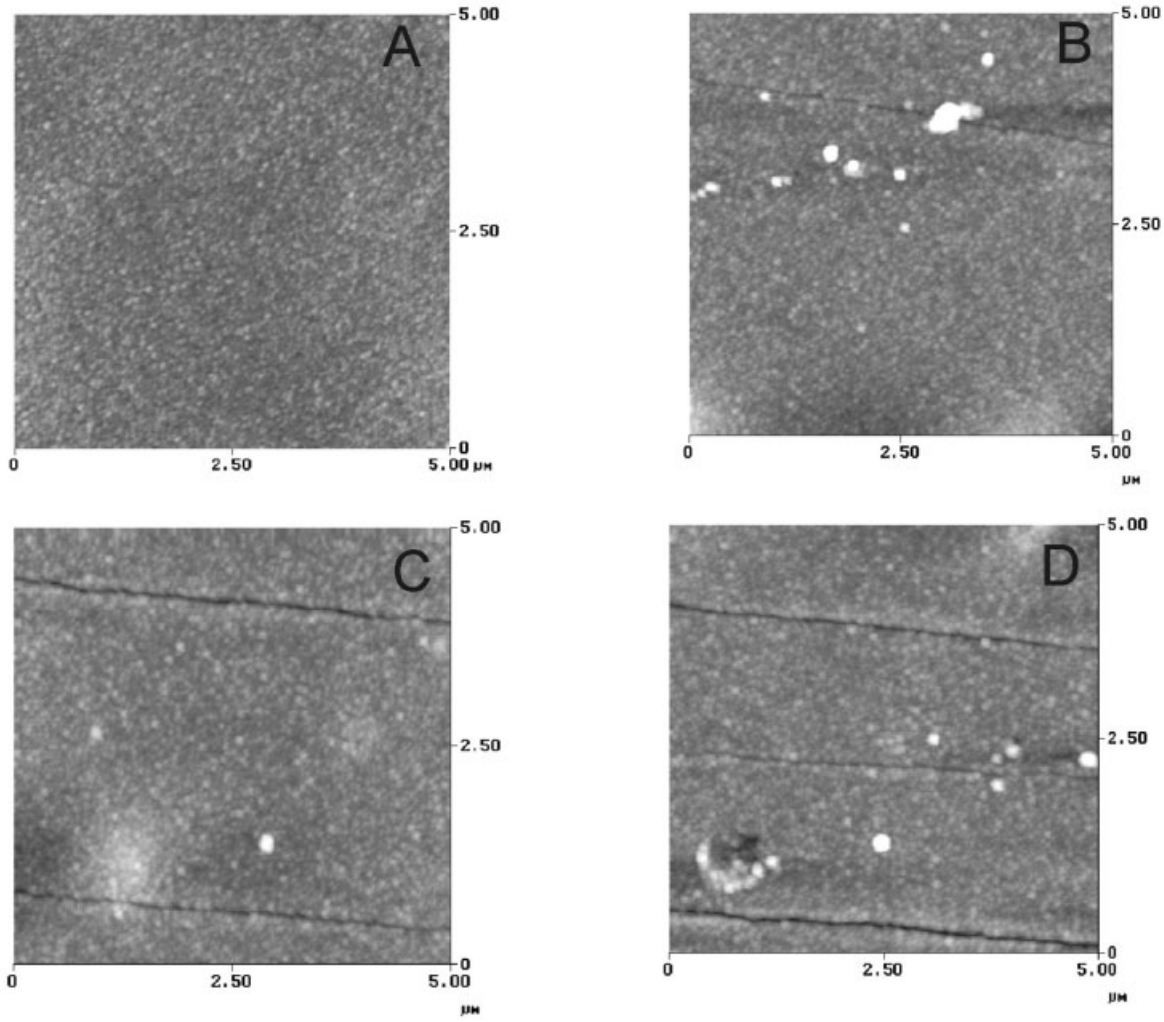

Figure 14 AFM images of the coating layers at different strains (a = 0%, b = 1%, c = 2%, and d = 3%)

value. When such a number becomes insignificant (above 2% strain), the E_p value for both-side–coated films becomes comparable to that of uncoated and single-side–coated PET films.

Surface morphology

It was found that, on stressing, parallel cracks appeared on the coating surface and the direction of the crack propagation was perpendicular to the direction of the stressing force. The same kind of observation also has been made on electron beam evaporated SiO_x coatings[19] and on RF plasma SiO_x coatings[2]. Another interesting point observed was that the extrusion direction of the PET film had no influence on the direction of crack propagation. Figure 13 shows the nature of cracks developed at approximately 2% strain in the single-side–coated film. The number of cracks was found to increase with increasing strain as is evident from the AFM images of the stressed films at different strains (Fig. 14). In macroscale, it appears that the cracks are very straight, but the high magnification AFM imaging reveals that the cracks propagate along the boundary of the deposited particles and not at all straight in microscale. Rather, they propagate in a zigzag manner (Fig. 15). The interparticle regions are the weakest regions in the coating layer along which the propagating crack makes its way.

CONCLUSION

The oxygen barrier properties of SiO_x type coatings are strongly dependent on the chemical composition and the surface morphology of the coating layer. In the present work, it was observed that higher oxygen flow rates and microwave power input during the coating process, within the working range, improve these properties. The presence of defects and their density play the major role in determining the barrier performance and its temperature dependence. Though SiO_x type coatings on PET films significantly improve their oxygen barrier performance, activation energy of permeance through the coated films indicates that the mechanism of oxygen permeation is similar through the uncoated and the single-side–coated films. The proposed model suggests that there exists a critical defect density below which the coating layer controls the kinetics of the permeation process. Above this critical density, the defect-free coating regions act as islands on the surface of the substrate (PET), which act as physical blocks on the paths of permeating molecules. In the both-side–coated films, there is a significant portion of the permeating molecules that permeate through the defect-free region of the coating layer at least on one side of the PET film. This is reflected in the substantial increase in the activation energy of oxygen permeation. Barrier performance deteriorates with straining of the films and, after a certain critical strain, it fails completely. However, in the strain region, where the barrier property fails, the similar behavior of the uncoated and coated PET films indicates that the changes in substrate layer (PET) also play an important role. Below this strain region, the lowering of E_p and oxygen permeance is mainly due to the appearance of cracks and perhaps the widening of the existing defects in the coating layer. The cracks run parallel to each other and are independent of the extrusion direction of the PET film. The interparticle regions are found to be the weak

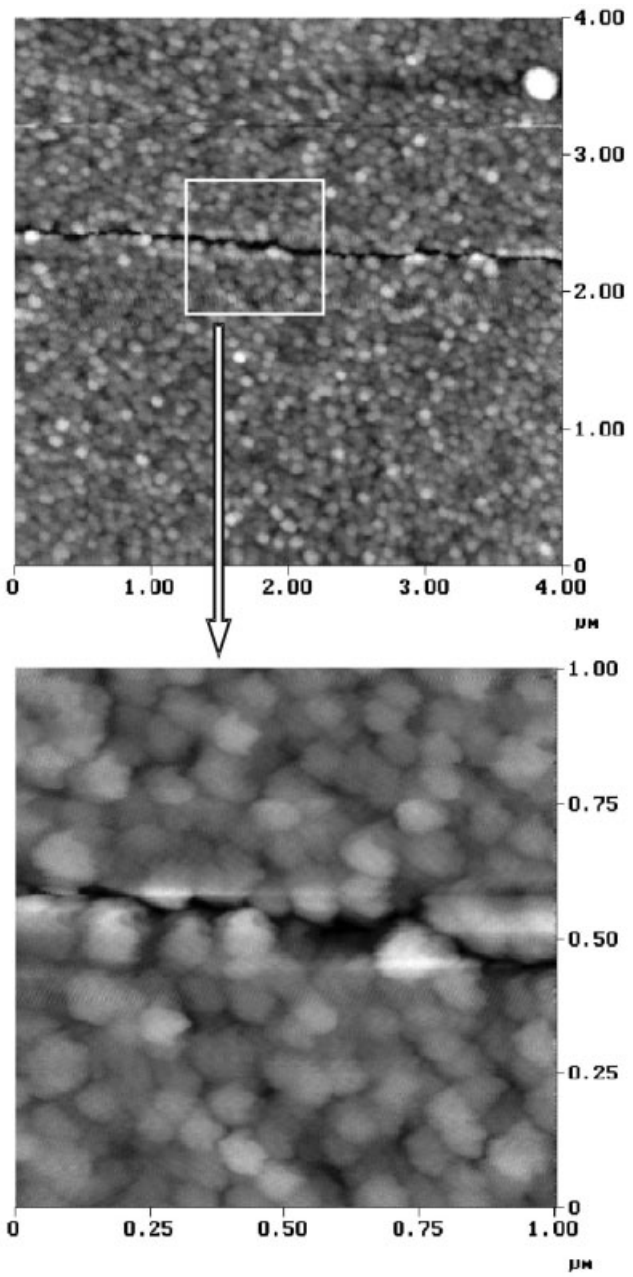

Figure 15 High magnification AFM image showing the nature of the crack propagation in a stressed coated film.

regions through which cracks propagate. Therefore, the ability of the SiO_x type of coatings to maintain a satisfactory oxygen barrier property against mechanical stress is mostly dependent on interfacial strength of the deposited particles.

These investigations were carried out with the financial support of Deutsche Forschungsgemeinschaft (DFG) and Deutscher Akademischer Austauschdienst (DAAD), to whom we extend our thanks.

References

1. Felts, J. T. 34th Annual Technical Conference Proceedings; Society of Vacuum Coaters, 1991, 99.
2. Heil, R. B. 38th Annual Technical Conference Proceedings; Society of Vacuum Coaters, 1995, 33.
3. Tropsha, Y. G.; Harvey, N. G. J Phys Chem B 1997, 101, 2259.
4. Inagaki, N.; Tasaka, S.; Hiramatsu, H. J Appl Polym Sci 1999, 71, 2091.
5. Hearvy, B. M.; Dineli, F.; Zhao, K. Y.; Grovenor, C. R. M.; Kolosov, O. V.; Briggs, G. A. D.; Roberts, A. P.; Kumar, R. S.; Howson, R. P. Thin Solid Films 1999, 355–356, 500.
6. da Silva Sobrinho, A. S.; Latreche, M.; Czeremuszkin, G.; Klemberg-Sapieha, J. E.; Wertheimer, M. R. J Vac Sci Technol A 1998, 16, 3190.
7. da Silva Sobrinho, A. S.; Czeremuszkin, G.; Latreche, M.; Wertheimer, M. R. J Vac Sci Technol A 2000, 18, 149.
8. Erlat, A. G.; Spontak, R. J.; Clarke, R. P.; Robinson, T. C.; Haaland, P. D.; Tropsha, Y. G.; Harvey, N. G.; Vogler, E. A. J Phys Chem B 1999, 103, 6047.
9. Wang, B.-C.; Tropsha, Y.; Montgomery, D. B.; Vogler, E. A.; Spopntak, R. J. J Mater Sci Lett 1999, 18, 311.
10. Dahlmann, R. Dissertation at RWTH Aachen University, 2001.
11. Roberts, A. P.; Henry, B. M.; Sutton, A. P.; Grovenor, C. R. M.; Briggs, G. A. D.; Miyamoto, T.; Kano, M.; Tsukahara, Y.; Yanaka, M. J Membr Sci 2002, 208, 75.
12. Rossi, G.; Nulman, M. J Appl Phys 1993, 74, 5471.
13. Kuhr, M.; Bauer, S.; Rothaar, U.; Wolf, D. Thin Solid Films 2003, 442, 107.
14. Garcia-Ayuso, G.; Vazquez, L.; Martinez-Duart, J. M. Surf Coat Technol 1996, 80, 203.
15. Barker, C. P.; Kochem, K. H.; Revell, K. M.; Kelly, R. S. A.; Badyal, J. P. S. Thin Solid Films 1995, 259, 46.
16. Mallik, R. R.; Henriksen, P. N.; Butler, T.; Kulnis, W. J.; Confer, T. J. J Vac Sci Technol A 1992, 10, 2412.
17. Thyen, R.; Weber, A.; Klages, C. P. Surf Coat Technol 1997, 97, 426.
18. Alexander, M. R.; Short, R. D.; Jones, F. R.; Michaeli, W.; Stollenwerk, M.; Mathar, G.; Zabold, J. Ceramic Films and Coatings; British Ceramic Proceedings No. 54; Institute of Materials: London, 1995; p 87.
19. Felts, J. T. 36th Annual Technical Conference Proceedings; Society of Vacuum Coaters, Dallas, 1993, 324.
20. Michaeli, W.; Göbel, S.; Costa, F. R. Strain Behavior of Plasma-Polymerized Permeation Barrier Layers on Plastics Films; Proceedings of the 18th Annual Meeting of the Polymer Processing Society, Guimarães, Portugal 2002.
21. Wagner, C. D.; Riggs, W. M.; Davis, L. E.; Moulder, J. F.; Muilenberg, G. E. Handbook of X-Ray Photoelectron Spectroscopy; Perkin Elmer Corp.: Eden Prairie, Minnesota, 1979.
22. Alexander, M. R.; Jones, F. R.; Short, R. D. J Phys Chem B 1997, 101, 3614.
23. Inagaki, N.; Tasaka, S.; Makino, M. J Appl Polym Sci 1997, 64, 1031.
24. Glastone, S.; Laidler, K. J.; Eyring, H. The Theory of Rate Processes; McGraw–Hill: New York, 1941.
25. Tropsha, Y. G.; Harvey, N. G.; Graper, J. C. Mater Res Soc Symp Proc 1997, 458, 403.
26. Yanaka, M.; Henry, B. M.; Roberts, A. P.; Grovenor, C. R. M.; Briggs, G. A. D.; Sutton, A. P.; Miyamoto, T.; Tsukahara, Y.; Takeda, N.; Chater, R. J. Thin Solid Films 2001, 397, 176.
27. This sample was prepared in a parallel research project with polycarbonate as substrate material on the same plant described in section 2.2, but with different process parameters (pressure: 30 Pa, coating time: 2 minutes, distance from plasma: 35 mm, HMDSO flow rate: 10 sccm, O_2 flow rate: 100 sccm).
28. The delamination of the coating from the epoxy resin and the pleating (dark lines) of the coating were caused by the sample preparation with an ultra cryo microtome.